Received: 24 March 2023 | Revised: 2 June 2023 | Accepted: 7 June 2023 | Published online: 8 June 2023

RESEARCH ARTICLE

Archives of Advanced Engineering Science
2023, Vol. 1(1) 55–62
DOI: 10.47852/bonviewAAES3202902

BON VIEW PUBLISHING

Performance Analysis of a Dynamic Test Bench Based on a Linear Direct Drive

Axel Wellendorf[1],* , Patrick Tichelmann[2] and Joachim Uhl[3]

[1]*Laboratory for Vibration Technology and Lightweight Constructions, Cologne University of Applied Sciences (TH Köln), Germany*

[2]*Laboratory for Applied Artificial Intelligence, Cologne University of Applied Sciences (TH Köln), Germany*

[3]*SCEMTEC Sensor Technology GmbH, Germany*

Abstract: This paper describes the design and performance of a dynamic test bench used for dynamic testing of special sensor systems intended for use in vehicle chassis. In order to economically meet all requirements of a dynamic driving simulation, the dynamic test bench is being developed on the basis of a linear direct drive. The test bench has a modular design and can be used flexibly, that is, vertically or horizontally. No ferromagnetic material is used in the measuring range of the sensor to minimize measurement inaccuracies. The performance requirements to be met are to the achievable acceleration and frequency, the stroke distance and the positioning accuracy. The test bench must be capable of accelerating at a minimum of 30 g while realizing an oscillation of at least 12 Hz. Regardless of the dynamic requirements, a minimum stroke distance of 500 mm is required. The required positioning accuracy is 1 mm. To ensure that all requirements are met, the performance limits of the test bench are determined experimentally and validated mathematically. In addition to the maximum acceleration and the maximum realizable frequency, the maximum stroke speed of the test rig is determined. Furthermore, the critical resonance frequencies of the test bench, which can lead to disturbances, are determined. As a result, all required performance values are exceeded by the dynamic test bench.

Keywords: dynamic test bench, linear direct drive, vibration technology, FEM, sensor testing

1. Introduction

Test benches are used to simulate physical reactions on a test specimen. There are a large number of vibration and dynamic test benches for different applications. The important parameters of vibration and dynamic test benches are nominal force or payload, frequency range, amplitude, velocity and acceleration. These parameters are physically interdependent and cannot reach their maximum values simultaneously. For this reason, test benches are designed for specific applications. Depending on the type of drive used, they can be classified as hydraulic, pneumatic or electromagnetic (Ausderau, 2004). Electromagnetic linear drives are also suitable for generating linear oscillating movements. A differentiation is made between linear direct drives and drives with transmission (Ausderau, 2004). Hydraulic test benches are widely used for industrial testing. Due to their high power density as well as large realizable forces and speeds, they are particularly suitable for large structures with high loads at low costs compared to other types of drives (Czichos, 2015; Gizatullin & Edge, 2007; Jovanovic et al., 2016; Tang et al., 2015). They can be used, for example, to test building structures and vehicles (Gizatullin and Edge, 2007; Ma et al., 2015; Rosti et al., 2022; Tang et al., 2015). However, hydraulic actuators are prone to leakage, which can pollute their environment. In addition, the compression of the working fluid by means of a pump generates noise (Czichos, 2015; Thomas, 2003). The positioning accuracy of hydraulic actuators is inferior to that of electrodynamic actuators. This is due to the large breakaway forces during the start of movement (Bruns et al., 2016; Bhagwat & Dey, 2022). Exemplary hydraulic test benches have one or more axes and can achieve payloads up to 14 t, frequencies up to 500 Hz, stroke distances up to 400 mm and accelerations up to 60 g (IABG, 2021; MTS Systems Corporation, 2018; Nelson, 2002).

Electro-hydraulic test benches have high precision. They are self-contained systems and do not require an external pressure supply by means of a separate pump (Gizatullin & Edge, 2007; Tang et al., 2015). Electro-hydraulic systems consist of an electric motor, an integrated hydraulic pump, a compact pressure tank and a hydraulic actuator (Jovanovic et al., 2016). Due to the nonlinear properties of the system caused by valve dynamics, dead zones, friction, etc., they are complex to control in order to compensate for these nonlinearities (Helian et al., 2020; Hao et al., 2022; Yao et al., 2014; Jovanovic et al., 2016; Tang et al., 2015; Yao et al., 2012, 2017). Electro-hydraulic actuators are used in injection molding machines and active vehicle suspensions (Helian et al., 2020; Yao et al., 2017). For small loads, these systems are not economical due to their size and the many components required.

*Corresponding author: Axel Wellendorf, Laboratory for Vibration Technology and Lightweight Constructions, Cologne University of Applied Sciences (TH Köln), Germany. Email: axel.wellendorf@th-koeln.de

Typical pneumatic drives achieve speeds in the range of 0.2 to 1 m/s. Higher speeds of up to 10 to 15 m/s can be achieved by so-called impact or high-speed pneumatic drives (Barycki et al., 2004). Servopneumatic actuators are used in many industrial applications because they are durable, robust and mechanically simple. In addition, their cost is low and, with air as their working fluid, they do not pollute their environment (Czichos, 2015; Göttert & Neumann, 2007; Hildebrandt et al., 2010; Thomas, 2003). They consist of a pneumatic actuator controlled by valves, a controller and reference sensors that measure the position, speed, acceleration and pressure (Thomas, 2003). For their operation, an external supply of compressed air, for example by a compressor, is required.

Compared to hydraulic and electric drives of the same size, pneumatic drives have a low force change gradient. As a result, their positioning dynamics are relatively low (Hildebrandt et al., 2010). In addition, pneumatic actuators are difficult to control because they exhibit significant nonlinearities (Czichos, 2015; Hildebrandt et al., 2010; Thomas, 2003). These are caused by the compressibility of the pressurized air, the nonlinear flow characteristics of the servo valve and the high static friction forces due to the sealing ring of the cylinder (Hildebrandt et al., 2010; Thomas, 2003). Air is highly compressible, which makes the actuator more flexible rather than stiff and results in a response delay. The stiffness of a linear air cylinder is position-dependent (Thomas, 2003). Due to low (inherent) stiffness and considerable friction forces, the positional accuracy is low compared to electric and hydraulic servo drives. The typical static position accuracy of servopneumatic drives is about ±0.2 mm (Hildebrandt et al., 2010). To improve the precision driving and control accuracy of pneumatic actuators, a double-chip piezoelectric oscillator as a driving source can be implemented (Liu et al., 2022). Electrodynamic shakers are comparatively inexpensive, easy to control, and behave approximately linearly. They generate oscillations by the means of a coil which is influenced by a magnetic field. When a current flows through the coil, the coil moves relative to the magnetic field. A force is induced, which is transmitted to the test specimen via a mounting device, for example a table with drilling pattern (Czichos, 2015; Colford et al., 2021; Lang, 1997; Lang & Snyder, 2001). Electrodynamic shakers are limited by their maximum amplitude at low frequencies, by their maximum velocity at medium frequencies and by their maximum acceleration or force at high frequencies (Colford et al., 2021). Exemplary shakers achieve maximum accelerations of more than 100 g and maximum velocities of more than 4 m/s in a frequency band of 2 to 25,000 Hz, with a stroke distance of less than 100 mm (Colford et al., 2021; Czichos, 2015).

In the case of a drive with transmission, the rotational movement of an electromagnetic drive is converted into a linear movement via a transmission. Rack and pinion, toothed belts or spindles are suitable for this purpose (Ausderau, 2004). By the means of the transmission, the load can be adjusted in terms of the drive forces and speeds, so that the rotary drive only needs to be designed in terms of its maximum power. Due to the mechanical clearance, the additional mass and the elasticity of the transmission, the positioning accuracy and the operating behavior are negatively affected. In addition, the transmission causes mechanical losses, operating noise and wear (Ausderau, 2004). Therefore, linear drives with transmission are not suitable for the dynamic test bench.

Linear direct drives achieve high stiffness and positioning accuracy because the linear motion is generated directly via the movement of a slider in a stator by a magnetic field (Ausderau, 2004; Budig, 2000; Schulze & Hauswald, 2005; Quang & Quang, 2021). They are used in particular for linear movements with high speeds and accelerations (Röhrig, 2004; Yi et al., 2022). Mechanical losses, operating noise and wear are reduced compared to drives with transmission (Ausderau, 2004). Stroke distances > 1 m, speeds > 4 m/s and accelerations of > 30 g can be achieved by the means of direct linear drives (Budig, 2000; Zhao & Xu, 2014).

To describe the dynamic behavior of a vehicle chassis, preliminary investigations have shown that accelerations of up to 30 g ($1g = 9.81\ m/s^2$) can occur when driving on an uneven road or through potholes. Vibrations with a maximum frequency of 12 Hz occur. A positioning accuracy of less than 1 mm is desired for examination of the sensors. In addition, maximum stroke distance of up to 500 mm is required. Another requirement for the test bench is the avoidance of ferromagnetic material in the area of the sensors, so that inductive measurement is not influenced. The payload for testing the sensor system is the sensor and can be specified as 0.2 kg. A portable and modular design with a flexible orientation (horizontal and vertical) is desired, as the test bench will be used for further dynamic investigations outside of this research project. Linear direct drives are particularly suitable for implementing the requirements to be met. Alternative drive types can only partially achieve the given dynamic requirements due to their design, are not suitable for portable use due to their size or are over-dimensioned for the payload of 0.2 kg. In the following, the design of the dynamic test bench based on the linear direct drive is described, and the physical limits of the test bench are determined experimentally and compared with the requirements to be met for chassis simulation.

2. Design of the Dynamic Test Bench Based on a Linear Direct Drive

The linear direct drive shown in Figure 1 is based on synchronous operation. The permanently magnetized slider is synchronously driven by a moving magnetic field in the stator (Schulze & Hauswald, 2005). The neodymium magnets responsible for this effect are located in the movable slider, while

Figure 1
Sectional view of a direct drive (LinMot, 2020)

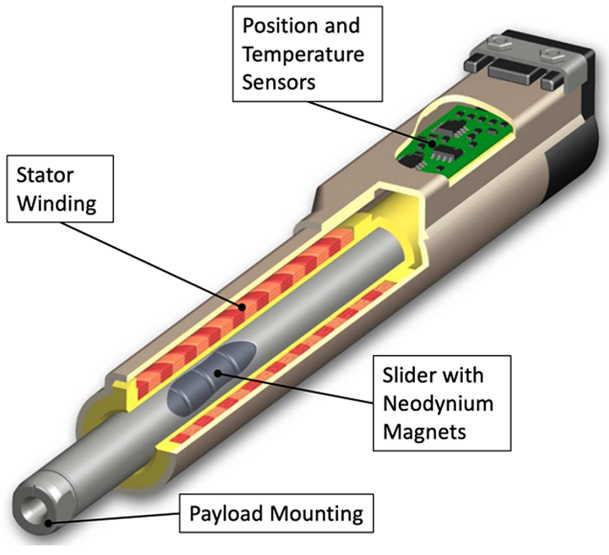

the windings are located in the passive stator. The stator also serves as a bearing for the slider.

Using an integrated displacement sensor system, which detects the magnetic field lines of the magnets in the slider by means of a Hall sensor, the relative position between the slider and the stator can be determined and controlled (LinMot, 2020).

The dynamic test bench examined in this contribution is an in-house development and represents a suitable, low-cost option for generating highly dynamic movements. With this dynamic test bench, both harmonic oscillations and user-defined curves, such as already recorded displacement/time curves from driving data, can be used to test sensor systems in a practical manner during development.

The dynamic test bench is designed with regard to the following requirements, which have been defined on the basis of typical driving curves:

- generation of movement with a frequency of at least 12 Hz
- payload (mount with sensor) of at least 0.2 kg
- acceleration of at least 30 g with payload
- velocity of at least 4 m/s
- stroke distance of at least 500 mm
- positioning accuracy of at least 1 mm within 500 mm stroke distance
- modular and portable design
- horizontal and vertical movement generation
- Inexpensive

Figure 2 shows the horizontal and vertical setup of the dynamic test bench. Relevant assemblies and components are numbered and briefly explained below.

- The control unit is required for controlling the linear unit and can be programmed with a PC so that user-defined traverse curves can be transferred and executed (LinMot, 2021).
- The stop plate is a steel plate mounted on silicone dampers that is attached to the frame. It is used to define machine zero (MagSpring, 2020).
- The frame consists of aluminum construction profiles (shown as gray profiles in Figure 2). Profiles made of wood fiber-PP composite are installed in the measuring area (shown as black profiles in Figure 2) to avoid interactions between electromagnetic fields of inductive sensors due to ferromagnetic components.
- The linear drive consists of the main stator/slider component (PS10-70x320U-BL-QJ/530) and is enclosed by a fluid cooling flange. This dissipates heat generated by power dissipation at the copper windings, which can occur during endurance tests. The positioning accuracy of the linear drive is 0.1 mm (LinMot, 2020).
- The dynamic sensor mount is attached to the slider and allows sensors to be attached. The sensor mount is supported in the underlying profile, preventing deflection or rotation of the slider during operation.
- The static sensor mount is aligned parallel to the dynamic sensor mount and is fixed at the end of the measurement range.
- The frame is fixed to eight modular, solid support feet, which prevent the test bench from moving at high dynamic forces. Despite a total weight of 380 kg, the test bench is portable due to the modular design and the demountable support feet.

3. Results and Discussion

In order to verify the applicability of the test bench to the requirements to be met, the performance limits are measured and compared with the requirements set. The following parameters are determined on the basis of test series:

- maximum velocity vmax
- maximum acceleration a_{max}
- maximum frequency f_{max} depending on the amplitude
- resonance frequency ranges of the dynamic test bench

Figure 2
Dynamic test bench

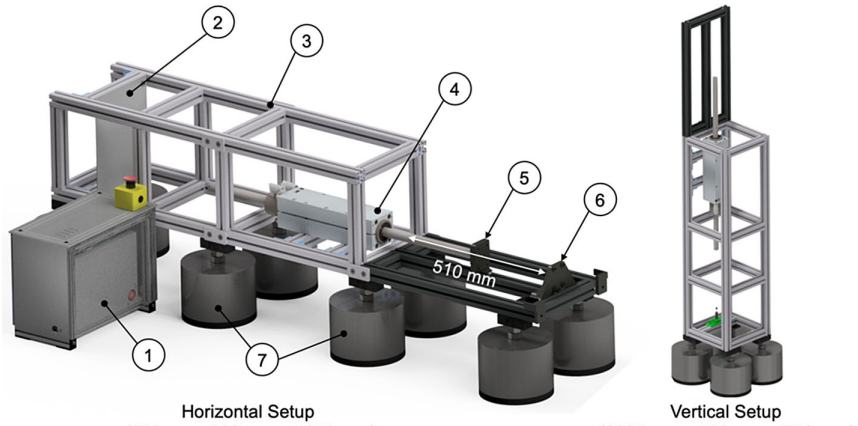

The parameters are measured by sensors integrated in the linear drive and external sensors attached to the test bench. The stator is equipped with sensors for position and speed measurement. These internal sensors are used to control and record the position and velocity.

To validate the internally measured parameters with the actual data at the sensor mount an external accelerometer is mounted to the test position (Figure 3). In this way, any deviations between the internally and externally measured parameters can be detected.

Figure 3
Dynamic test bench with mount of acceleration sensor (left) and flowchart for sensor testing (right) time

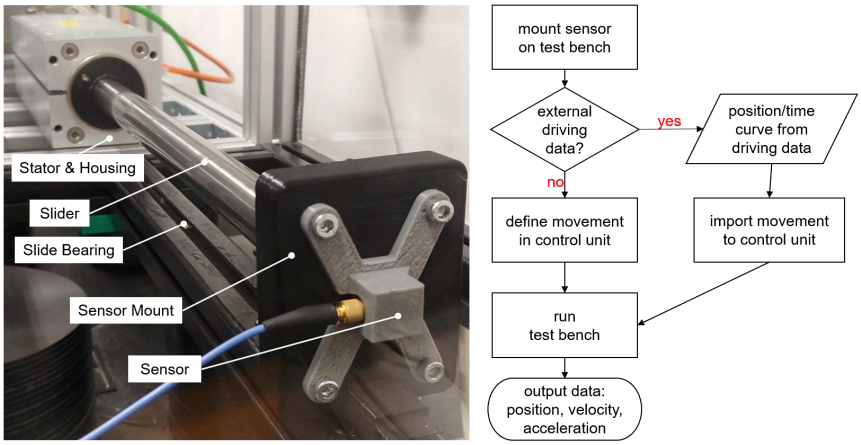

3.1. Maximum velocity as a function of displacement

In order to determine the maximum velocity vmax, point-to-point movements of different displacements s are programmed with the control software and sent to the control unit. The maximum velocity of the respective defined displacement vmax i is recorded and evaluated with the internal sensor system (MagSpring, 2020).

The test results in Figure 4 show the maximum measured velocity vmax i as a function of the displacement.

The results show that the maximum velocity of the dynamic test bench is reached at a displacement of 210 mm. It is $v_{max} = 5.6$ m/s. In the range from 60–210 mm, the curve does not show a linear, but a degressive progression.

Figure 4
Maximum velocity plotted against displacement with a payload of 0.2 kg

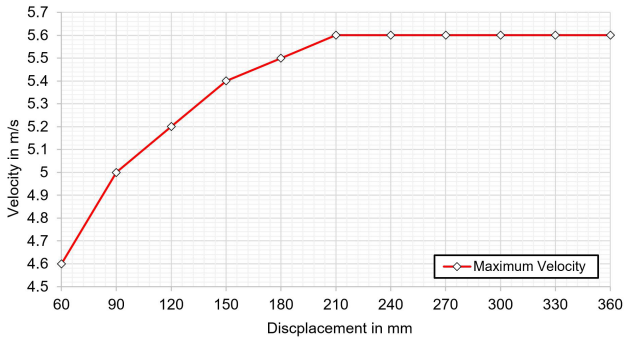

3.2. Maximum acceleration as a function of displacement

To determine the maximum acceleration a_{max}, point-to-point movements with different displacements s are executed by the dynamic test bench as described in the previous section. The limitation of the maximum acceleration is removed in the software. Starting from 10 mm, the displacement s is increased stepwise by 10 mm.

Figure 5 shows an exemplary acceleration curve as a function of time for a displacement of 60 mm. The maximum acceleration and the time to reach the maximum acceleration Δt are determined from the acceleration curve.

Figure 5
Acceleration plotted against time at a displacement of 60 mm with a payload of 0.2 kg

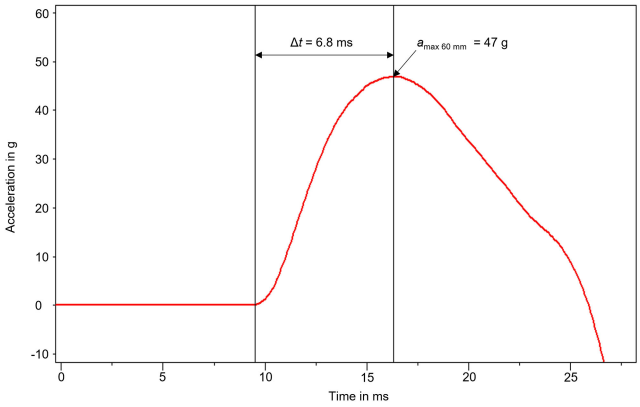

The accelerations of the defined displacements s are measured with an external, single-axis acceleration sensor Type 352C04. The values of the maximum measured accelerations a_{max} *i* of the respective displacements and the times to reach the maximum accelerations Δ*t i* are summarized in Figure 6.

Figure 6
Maximum acceleration and time to reach maximum acceleration plotted against displacement with a payload of 0.2 kg

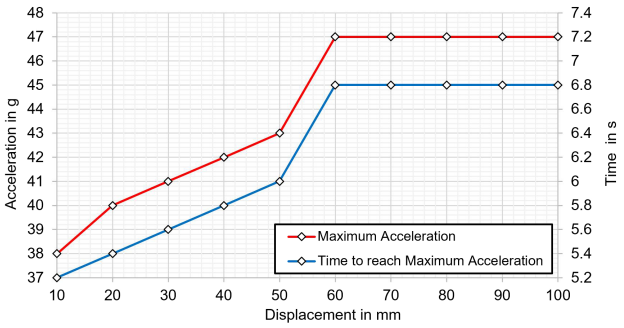

At displacements from 10 to 50 mm, the maximum acceleration a_{max} i increases approximately linearly. Between 50 and 60 mm displacement, there is a greater increase in a_{max} i from 43 to 47 g. If the displacement is greater than $s = 60$ mm, there is no further increase in maximum acceleration. This shows that the maximum achievable acceleration is $a_{max} = 47$ g at a displacement of 60 mm or greater.

The maximum acceleration a_{max} depends on the actual payload and can be calculated according to the equation:

$$a_{max} = \frac{F}{m_{slider} + m_{payload}} = \frac{2236N}{4.65\ kg + m_{payload}} \quad (1)$$

In experimental tests, the maximum acceleration a_{max} is confirmed for different payloads up to a payload of 1 kg with a deviation of max. 1.2 %. Thus, a payload of 0.2 kg results in a maximum acceleration of 47.00 g and a payload of 1 kg results in a maximum acceleration of 39.86 g.

3.3. Maximum frequency as a function of amplitude

To determine the maximum frequency as a function of amplitude, harmonically oscillating movements are generated with the test bench. These experiments show that the maximum acceleration of the test rig is achievable at small amplitudes, in contrast to the point-to-point movements in the previous sections where the maximum acceleration depends on the displacement. However, the previously determined maximum velocity v_{max} von 5.6 m/s and maximum acceleration a_{max} of 47 g also apply to this type of motion.

Assuming harmonic oscillation, the maximum achievable frequency f as a function of amplitude $\hat{x}$ at constant maximum acceleration a_{max} can be described by the following equation.

$$f(\hat{x})_1 = \frac{\sqrt{\frac{a_{max}}{\hat{x}}}}{2\pi} \quad (2)$$

with

$$a_{max} = \hat{x} \cdot \omega^2 \quad (3)$$

and

$$\omega = 2\pi \cdot f \quad (4)$$

In this case, the maximum speed increases constantly with the frequency. If the maximum speed of the dynamic test bench is reached, then the maximum achievable frequency f must be calculated as a function of the amplitude $\hat{x}$ using the following equation.

$$f(\hat{x})_2 = \frac{v_{max}}{2\pi \cdot \hat{x}} \quad (5)$$

with

$$v_{max} = \hat{x} \cdot \omega \quad (6)$$

and

$$\omega = 2\pi \cdot f \quad (7)$$

Based on the test data $a_{max} = 47$ g and $v_{max} = 5.6$ m/s, the diagram shown in Figure 7 is created. It shows the theoretically achievable frequencies and velocities of a harmonically oscillating motion as a function of amplitude.

Up to the amplitude $\hat{x}_{cut} = 68.025$ mm, the acceleration is constant and the velocity increases steadily. At an amplitude greater than 68.025 mm, the maximum velocity is reached and remains constant. For this reason, the acceleration decreases at amplitudes greater than 68.025 mm. The amplitude $\hat{x}$cut can be calculated with the following equation.

$$\hat{x}_{cut} = \frac{(v_{max})^2}{a_{max}} = \frac{(5,6\,\frac{m}{s})^2}{461\,\frac{m}{s^2}} = 68.025\ mm \quad (8)$$

All frequency-amplitude combinations shown in the light gray colored area can be achieved by the test bench. With an amplitude $\hat{x} = 50$ µm, the linear drive reaches a maximum frequency of 483.302 Hz. With the maximum displacement of the linear drive of 510 mm, the amplitude is 255 mm at a maximum frequency of 3.5 Hz.

This diagram of the dynamic test bench for harmonic vibrations is confirmed by experimental tests. Table 1 shows excerpts of the calculated and experimentally determined maximum frequencies

Figure 7
Maximum frequency and maximum velocity plotted against amplitude with a payload of 0.2 kg

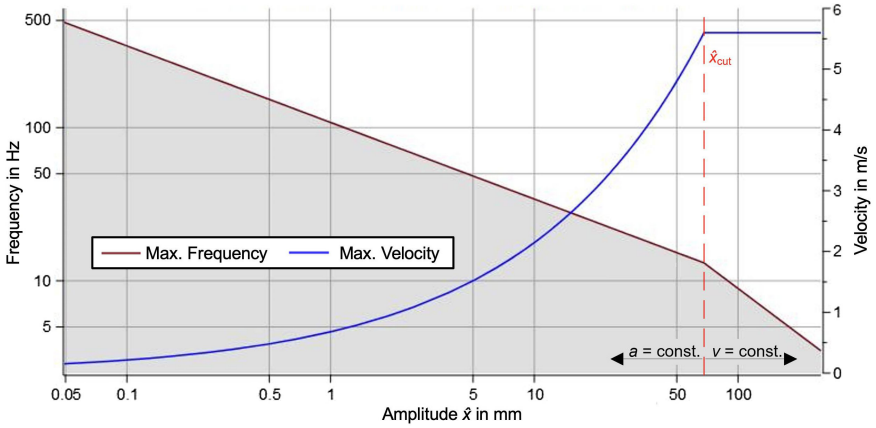

Table 1
Calculated and experimentally measured maximum frequencies as a function of the amplitude

$\hat{x}$ *[mm]*	*f* calculated [Hz]	*f* measured [Hz]	Difference [Hz]
0.05	483.3	482	1.3
52	14.99	14.9	0.087
60	13.95	13.9	0.052
68	13.11	13.1	0.0054
200	4.361	4.3	0.16

as a function of the amplitude. Above these determined frequencies shown, the dynamic test bench cannot be operated.

The results show that the determined limit values correspond with reality.

3.4. Resonance ranges

FEM modal analyses are carried out to determine the structural resonances of the dynamic test bench. The FEM modal analysis shows that natural modes affecting the measuring area (slider and front of frame) occur at the following frequencies.

- 73.177 Hz
- 89.016 Hz
- 125.72 Hz
- 127.82 Hz
- 145.66 Hz

No resonance frequencies are determined below 73.17 Hz. Above 145.66 Hz, resonance frequencies occur in the frame outside the measuring area. These frequencies do no effect the measuring area of the test bench. Figure 8 shows the first natural mode of the test bench at 73.177 Hz. Here, the front part of the slider oscillates in radial direction. The resonance ranges can be confirmed experimentally.

3.5. Discussion

Figure 9 summarizes the results of the performance analysis of the dynamic test bench with a payload of 0.2 kg. The feasible frequency-amplitude combinations are colored gray, and the red colored areas represent the resonance ranges and are to be avoided.

Figure 8
First mode of the test bench at 73.177 Hz

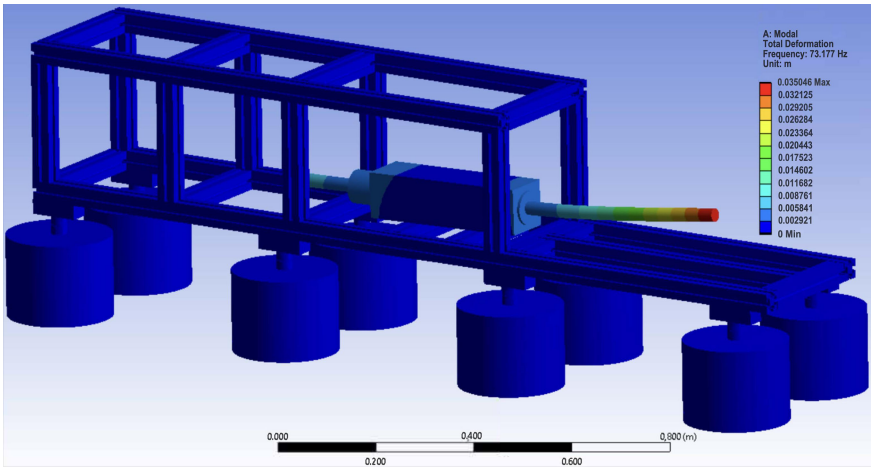

Figure 9
Maximum frequency and maximum velocity plotted against amplitude with a payload of 0.2 kg (resonance ranges marked in red)

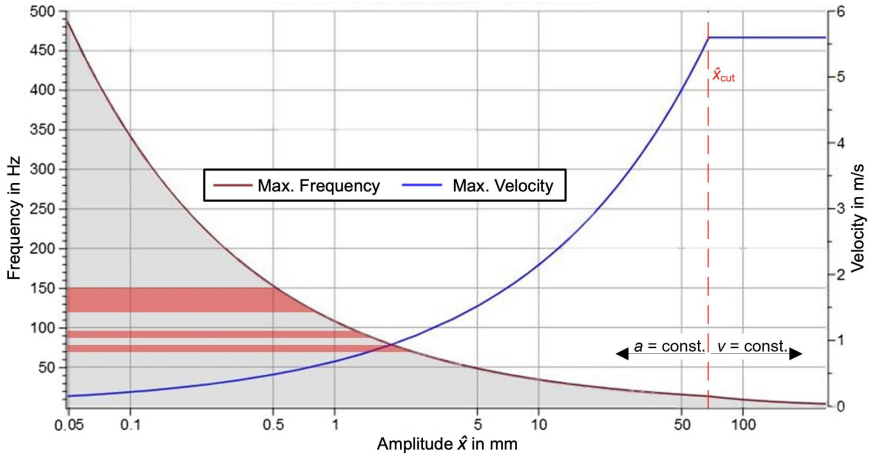

Table 2
Performance limits

Maximum stroke distance (amplitude $\hat{x}$)	510 mm (255 mm)
Maximum frequency (at $\hat{x} = 0.05$ mm)	483 Hz
Maximum frequency (at $\hat{x} = 50$ mm)	15.3 Hz
Maximum frequency (at $\hat{x} = 255$ mm)	3.5 Hz
Maximum acceleration (with 0.2 kg payload)	47.00 g
Maximum acceleration (with 1.0 kg payload)	39.86 g
Maximum velocity	5.6 m/s
Positioning accuracy	0.1 mm

The results show that the dynamic test bench meets all specifications required for the dynamic driving simulation. Due to the lightweight, modular design, the test bench can be operated horizontally or vertically at different locations. Table 2 shows the performance limits of the test bench.

4. Conclusion

This paper describes the design and operation of a dynamic test bench based on a linear direct drive. The test bench is designed for dynamic testing of light sensor systems intended for use in vehicle chassis. The basis is the acceleration data recorded in a real driving test on chassis of different vehicle classes. These driving tests can be simulated in the laboratory with the dynamic test bench in order to test the sensor systems efficiently.

The test bench can be operated at frequencies of up to 483 Hz. The maximum amplitude of the test bench is 255 mm. It achieves a maximum stroke distance of 510 mm. The maximum acceleration with a payload of 0.2 kg is 47 g. It represents the limit of the frequency-amplitude range up to an amplitude of 68 mm. Above 68 mm, the max. velocity of 5.6 m/s is reached and the acceleration decreases.

This test bench is freely programmable, and dynamic driving simulations can be performed. Beside measuring and calibrating the accuracy of special sensor systems for use in vehicle chassis, this multi-usable and portable test bench can be set up for standard or newly developed dynamic tests within its performance limits.

Acknowledgements

This work was financially supported by Zentrales Innovationsprogramm Mittelstand (ZIM) of the Bundesministerium für Wirtschaft und Energie (BMWi) (16KN081724).

Conflicts of Interest

The authors declare that they have no conflicts of interest to this work.

References

Ausderau, D. (2004). Polysolenoid-linearantrieb mit genutetem stator. *Doctoral Thesis*, *Swiss Federal Institute of Technology*. https://doi.org/10.3929/ethz-a-004714429

Barycki, J., Ganczarek, M., Kollek, W., Mikulczynski, T., & Samsonowicz, Z. (2004). Performances of high-speed pneumatic drive with self-acting impulse valve. *Mechanism and Machine Theory*, *39*(6), 657–663. https://doi.org/10.1016/S0094-114X(03)00089-2

Bhagwat, M., & Dey, A. K. (2022). Delay compensation in high speed hydraulic control systems to improve system stability. *In IEEE 2022 4th International Conference on Electrical, Control and Instrumentation Engineering (ICECIE)*, 1–4.

Bruns, P., Mojrzisch, S., Twiefel, J., Wallaschek, J., Zimmermann, U., & Klie, W. (2016). Prüfstand mit piezoelektrischen Schwingungserzeugern zur Ermittlung der dynamischen Steifigkeit von Elastomerbauteilen (in German). *Forschung im Ingenieurwesen*, *80*, 29–40. https://doi.org/10.1007/s10010-016-0204-y

Budig, P. K. (2000). The application of linear motors. *In IEEE 2000 Third International Power Electronics and Motion Control Conference*, 1336–1341. https://doi.org/10.1109/IPEMC.2000.883044

Colford, G., Craft, K., Morello, A., Harvey, D., Haynes, C., & Taylor, S. (2021). Shaker-amplifier system characterization. *In Conference Proceedings of the Society for Experimental Mechanics Series,* 351–360. https://doi.org/10.1007/978-3-030-47709-7_33

Czichos, H. (2015). *Mechatronik: Grundlagen und anwendungen technischer systeme.* Germany: Springer Vieweg Wiesbaden. https://doi.org/10.1007/978-3-658-09950-3

Gizatullin, A. O., & Edge, K. A. (2007). Adaptive control for a multi-axis hydraulic test rig. *In 2007 Proceedings of the Institution of Mechanical Engineers, Part I: Journal of Systems and Control Engineering*, 183–198. https://doi.org/10.1243/09596518JSCE314

Göttert, M., & Neumann, R. (2007). Bahnregelung servopneumatischer Antriebe – ein Vergleich von linearen und nichtlinearen Reglern (Continuous Path Control of Servo Pneumatic Drives – A Comparison of Linear and Non Linear Controllers). *Automatisierungstechnik*, *55*(2), 69–74. https://doi.org/10.1524/auto.2007.55.2.69

Hao, Y., Quan, L., Qiao, S., Xia, L., & Wang, X. (2022). Coordinated control and characteristics of an integrated hydraulic–electric hybrid linear drive system. *IEEE/ASME Transactions on Mechatronics*, *27*(2), 1138–1149. https://doi.org/10.1109/TMECH.2021.3082547

Helian, B., Chen, Z., & Yao, B. (2020). Precision motion control of a servomotor-pump direct-drive electrohydraulic system with a nonlinear pump flow mapping. *IEEE Transactions on Industrial Electronics 67*(10), 8638–8648. https://doi.org/10.1109/TIE.2019.2947803

Hildebrandt, A., Neumann, R., & Sawodny, O. (2010). Optimal system design of siso-servopneumatic positioning drives. *IEEE Transactions on Control Systems Technology 18*(1), 35–44. https://doi.org/10.1109/TCST.2008.2009879

IABG (2021). Überblick Testanlagen. Retrieved from: https://www.iabg.de/fileadmin/media/Broschueren/AM/AUT_Ueberblick_Testanlagen_dt.pdf

Jovanovic, V., Djuric, A., Karanovic, V., & Stevanov, B. (2016). Applications of electro-hydraulics actuators. *In 2016 IEEE SoutheastCon*, 1–5. https://doi.org/10.1109/SECON.2016.7506678

Lang, G. F. (1997). Electrodynamic shaker fundamentals. *Journal of Sound and Vibration*, *31*(4), 14–23.

Lang, G. F., & Snyder, D. (2001). Understanding the physics of electrodynamic shaker performance. *Journal of Sound and Vibration, 35*(10), 24–33.

Liu, X., Wang, T., Wang, H., Hou, J., Liu, J., & Tian, X. (2022). Design and testing of piezoelectric pneumatic actuators. *In 2022 IEEE International Conference on Wireless Communications, Electrical Engineering and Automation (WCEEA)*, 97–102.

Ma, W., Song, R., Xu, J., Zang, Y., & Luo, S. (2015). A coupling vibration test bench and the simulation research of a maglev

vehicle. *Shock and Vibration*, *2015*. http://doi.org/10.1155/2015/586910

MTS Systems Corporation (2018). Multi-axial simulation table (mast) systems. Retrieved from https://www.mts.com/cs/groups/public/documents/library/dev_002251.pdf

Nelson, C. (2002). Vibration test evolution single-axis, single-shaker to 6DoF. Retrieved from: https://www.semanticscholar.org/paper/Vibration-Test-Evolution-Single-Axis-%2C-to-6-DoF/35d1d0b37d9bd1c15f2bd257ab525a7166524e67

NTI AG, LinMot (2020). Linearmotoren P10-70X320U. Spreitenbach.

NTI AG, LinMot (2021). Drive Serie E1400. Available. Spreitenbach.

NTI AG, LinMot, MagSpring (2020). LinMot-Talk 6 Configuration Software. Spreitenbach.

Quang, N. H., & Quang, N. P. (2021). Continuous control set model predictive control for polysolenoid linear motor. *Turkish Journal of Computer and Mathematics Education*, *12*(13), 2473–2478.

Röhrig, C. (2004). Linearmotoren sicher positioniert. *Antriebstechnik*, *43*(5), 50–56.

Rosti, M., Cii, S., Bussini, A., Calvi, P. M., & Ripamonti, F. (2022). Design and validation of a hardware-in-the-loop test bench for evaluating the performance of an active mass damper. *Journal of Vibration and Control, 29*(17–18). https://doi.org/10.1177/10775463221111262

Schulze, J., & Hauswald, T. (2005). *Neuartige und weiterentwickelte Bahnsysteme 2 – Linearmaschinen*. Germany: TU Berlin.

Tang, Y., Zhu, Z., Shen, G., & Li, X. (2015). Experimental investigation of feedforward inverse control with disturbance observer for acceleration tracking of electro-hydraulic shake table. *Journal of Vibroengineering*, *17*(1), 330–345.

Thomas, M. B. (2003). Advanced servo control of a pneumatic actuator. *Doctoral Dissertation*, *Ohio State University.*

Yao, J., Jiao, Z., & Ma, D. (2014). High dynamic adaptive robust control of load emulator with output feedback signal. *Journal of the Franklin Institute*, *351*(8), 4415–4433. https://doi.org/10.1016/j.jfranklin.2014.06.002

Yao, J., Deng, W., & Jiao, Z. (2017). RISE-based adaptive control of hydraulic systems with asymptotic tracking. *IEEE Transactions on Automation Science and Engineering 14*(3), 1524–1531. https://doi.org/10.1109/TASE.2015.2434393

Yao, J., Jiao, Z., & Yao, B. (2012). Robust control for static loading of electro-hydraulic load simulator with friction compensation. *Chinese Journal of Aeronautics 25*(6), 954–962. https://doi.org/10.1016/S1000-9361(11)60467-6

Yi, S. C., Chen, H., Jiang, Z., Xu, L., & Zhang, Q. (2022). Positioning and vibration control of a magnetostrictive-actuated stewart platform with hysteresis compensation. *In 2022 41st Chinese Control Conference (CCC)*, 2369–2374.

Zhao, Y. P., & Xu, Y. H. (2014). Electric Machine Technology Needs Analysis of the Linear Motor. *Applied Mechanics and Materials*, *490–491*, 1138–1141. https://doi.org/10.4028/www.scientific.net/amm.490-491.1138

How to Cite: Wellendorf, A., Tichelmann, P., & Uhl, J. (2023). Performance Analysis of a Dynamic Test Bench Based on a Linear Direct Drive. *Archives of Advanced Engineering Science* 1(1), 55–62, https://doi.org/10.47852/bonviewAAES3202902